Magn Reson Med Sci 2022; 21; 415–424
doi:10.2463/mrms.mp.2020-0154 Published Online: February 27, 2021

MAJOR PAPER

Susceptibility-weighted Imaging for Renal Iron Overload Assessment: A Pilot Study

Jun Sun[1], Yuanyuan Sha[1], Weiwei Geng[1], Jie Chen[1], and Wei Xing[1*]

Purpose: To explore the feasibility of susceptibility-weighted imaging (SWI) for evaluating renal iron overload.

Methods: Twenty-eight rabbits were randomly assigned into control (n = 14) and iron (n = 14) group. In the 0th week, the study group was injected with iron dextran. Both groups underwent SWI examination at the 0th, 8th, and 12th week. The signal intensity (SI) of cortex and medulla was assessed. Angle radian value (ARV) calculated with phase image was taken as the quantitative value for cortical and medullary iron deposition. After the 12th week, the left kidneys of rabbits were removed for pathology. The difference in the ARV among three groups was analyzed using Kruskal–Wallis test. The difference of the iron content between two groups was analyzed through independent sample *t*-test.

Results: In the iron group: at the 12th week, eight rabbits were found to have decreased SI of only cortex, and the other six rabbits had decreased SI of cortex and medulla by the same degree; the ARV of cortex at the 8th and 12th week was significantly higher than that of the 0th week ($P < 0.05$); the ARV of the six rabbits' medulla at the 12th week was significantly higher than that of the 0th week, 8th week, and the other eight rabbits at the 12th week ($P < 0.05$); at the 12th week, eight rabbits (iron group) were found to have many irons only deposit in the cortex, and the others were found to have many irons deposit in both cortex and medulla; the iron content of cortex and six rabbits' medulla in the iron group was significantly higher than that of the control ($P < 0.05$).

Conclusion: The ARV of SWI can be used to quantitatively assess the excess iron deposition in the kidneys. Excessive iron deposition mainly occurs in the cortex or medulla and causes their SWI SI to decrease.

Keywords: *iron deposition, kidney, susceptibility-weighted imaging*

Introduction

Iron is one of the essential microelements for organisms.[1,2] Under normal conditions, humans maintain the balance between absorption, use, and loss.[3] However, once the iron is excessive, the human body has no mechanisms to clear the excess iron.[4] Excess iron will deposit in some of the organs and is detrimental.[4] Kidney is one such organ which gets affected commonly. Iron overload has been affirmed as a dangerous factor for kidney dysfunction, which is associated with chronic kidney disease (CKD) caused by conditions like diabetic nephropathy, hypertensive kidney injury, and renal fibrosis.[3–6] It was reported that iron deposition was observed in the proximal and distal tubules of the kidney in human CKD.[5,7] Excessive iron promotes increased free radical generation and oxidative stress, which causes renal cellular and tissue damage.[5,7,8] On the other hand, dietary iron restriction or the treatment through chelating agents can alleviate renal iron overload, thereby inhibiting the progression of the pre-existing renal injury.[5,8,9] It follows that the degree of renal iron deposition is related to its injury. Accurate and effective evaluation of excessive iron deposition in the kidney is of great value in monitoring renal injury in CKD patients.[10]

At present, Prussian blue staining[9] can be used to analyze the distribution of excess iron deposition in the kidney, and atomic absorption spectrophotometer can be used to measure renal iron content. However, both the methods are invasive and require a tissue sample, which is not suitable for clinical follow-up monitoring of excessive iron deposition in the kidney for CKD

[1]Department of Radiology, The Third Affiliated Hospital of Soochow University, Changzhou, Jiangsu Province, China

[*]Corresponding author: Department of Radiology, The Third Affiliated Hospital of Soochow University, No. 185, Juqian Street, Tianning District, Changzhou 213003, Jiangsu Province, China. Phone: +86 13961236568, Fax: +86-0519-86621235, E-mail: suzhxingwei@suda.edu.cn

Received: July 30, 2020 | Accepted: December 29, 2020

patients. To address these requirements of safe, non-invasive, and ability to offer repeated evaluations for monitoring, MRI offers the possibility of a viable alternative through susceptibility-weighted imaging (SWI), an emerging functional MRI technique. It uses tissue magnetic susceptibility difference to generate a unique contrast that differs from that obtained with conventional MRI.[11,12] Combining the phase and magnitude images, SWI offers a good demonstration of paramagnetic signals.[13] Iron is a paramagnetic substance, as evidenced by its short T2 relaxation time.[10] It has been demonstrated that SWI can measure the tissue iron concentration reliably, which was consistent with the autopsy examination results.[14] Hence, SWI can be regarded as a reliable marker through tracking iron overload in various associated diseases, thereby analyzing progression.[10]

So far, SWI has been used to detect and quantify iron deposition in the liver[11] and brain[13,14] tissue. Even after an extensive literature search, the papers evaluating renal iron deposition were next to none. In this study, we used animal experiments to explore the value of SWI in the qualitative and quantitative detection of excessive iron deposition in the kidney, considering the results of Prussian blue staining and atomic absorption spectrophotometer as the reference standard.

Materials and Methods

This study was approved by the ethics committee of The Third Affiliated Hospital of Soochow University (Approval number: 2019026).

Animal modeling and grouping

We used Twenty-eight purebred healthy New Zealand white rabbits (provided by Suzhou Huqiao Biotechnology Limited Company, Suzhou, China), each weighing 2.0–2.5 kg, 2–3 months old, 16 males and 12 females, grown at a room temperature of 22°C, clean environment, fed with complete formula fodder, and purified water. All rabbits were randomly divided into the following two groups:

1. Iron group: 14 rabbits (7 males and 7 females). On the first day of the 0th week, after documenting the bodyweight, a suspension of iron dextran containing 20 mg/ml of iron was injected into the gluteal muscles at a dose of 3 ml/kg.
2. Control group: 14 rabbits (9 males and 5 females). No iron was injected.

MR examination

The schedule of MRI examination in the iron and control group is as follows: on the first day of the 0th, 8th, and 12th week, respectively.

To reduce the intestinal peristalsis artifacts, food intake was restricted for a period of 8 hours before the examination. Anesthesia was achieved by injecting 3% pentobarbital sodium solution into the hind leg muscles at a dose of 1 ml/kg before the scanning. During the examination, the head was entered first, and the left kidney was scanned while in the left lateral position. The scanning range was from the upper pole to the lower pole of the kidney. All MRI images were acquired on a 3.0 T MRI system (Magnetom Verio; Siemens Healthcare, Erlangen, Germany) with a standard eight-channel phase array body matrix coil. The MRI protocols are shown in Table 1. The sequence of SWI produced the final magnitude image, maximum intensity projection image, phase image, and SWI image.

Image analysis

All images were analyzed by two physicians with more than five years of work experience in the interpretation of abdominal MRI. At the syogo.via post-processing workstation (Siemens), they entered the viewing interface and simultaneously opened the T_2-weighted images (T_2WI), SWI, and phase sequences and selected the largest central level image of the kidney. The analysis was done as follows: (1) Qualitative analysis: On the T_2WI and SWI, the signal intensity (SI) of the renal cortex and medulla was observed. (2) Quantitative analysis: According to the T_2WI and SWI, the cortical region was manually delineated on the SWI at the central level of the kidney, avoiding the boundary area that may affect the signal value, so did the medulla. By applying the copy and paste function of the workstation, the cortical and medullary region in the SWI was, respectively, copied to the phase image. Then, the cortical and medullary region in the phase image was, respectively, divided into three sub-regions of roughly equal area, including the front, middle, and back (Fig. 1). The phase value was obtained by, respectively, drawing the region of interest in the three sub-regions manually. The average value of the three sub-regions phase value was taken for the phase value (X) of the entire renal cortex and medulla, respectively. The angle radian value (ARV) was calculated by the following formula: $ARV = (-X \times \pi)/4096$, and was utilized for the quantification of iron deposition, where X had a range from –4096 to 4095.[15] The unit of ARV is radian.

Pathological examination

After the 12th week MRI scan, all rabbits were still under anesthesia. At this time, all rabbits were sacrificed by air embolization, and left kidneys were removed. Enough tissues of the renal central level were sampled and fixed in 10% neutral buffered formalin. As per the routine protocol, tissues were dehydrated, made transparent, wax-impregnated, paraffin-embedded, sectioned, stained with hematoxylin-eosin and Prussian blue and evaluated for renal iron deposition under brightfield microscopy.

The remaining renal cortical and medullary tissues were sent to the Guangdong Medical Laboratory Animal Center, and measurement of the cortical and medullary iron content was done by atomic absorption spectrophotometer.

Table 1 Sequences and parameters of MRI protocols

Parameters	Conventional MRI		SWI
	T2-weighted HASTE		GRE
Plane orientation	Coronal	Transverse	Transverse
Acquisition type	2D	2D	2D
Repetition time (ms)	1400	1000	472
TE (ms)	93	108	14.8
Field of view (mm)	153 × 219	130 × 130	136 × 136
Matrix	126 × 256	179 × 256	269 × 384
Slice thickness (mm)	3	3	3
Inter-slice gap (mm)	0.9	0.6	0.6
flip angle (degrees)	160	138	20
Bandwidth (Hz/pixel)	781	199	70
Acquisition time	14 s	1 min and 38 s	6 min and 58 s

D, dimension; GRE, gradient-recalled echo; HASTE, half acquisition single-shot turbo spin-echo; Hz, Hertz; SWI, susceptibility-weighted imaging.

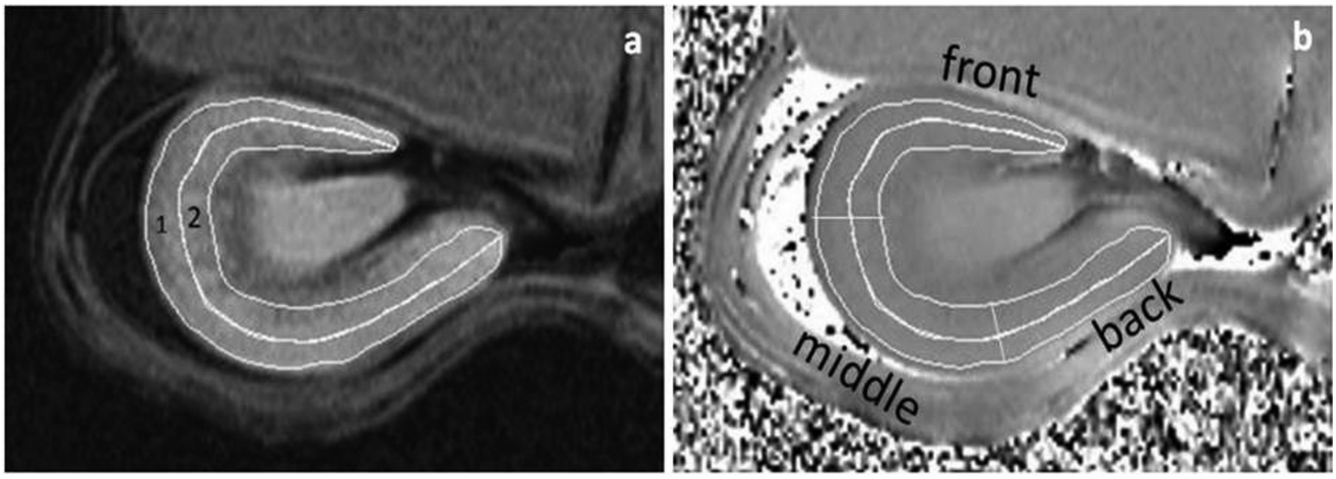

Fig. 1 Exemplification of the renal cortical (1 represents the contour of cortex) and medullary (2 represents the contour of medulla) region delineated and divided on SWI and phase image. On SWI image (**a**), the cortical region was manually delineated excluding the boundary area that may affect the signal value, so did the medulla. The cortical and medullary region on the SWI image was, respectively, copied and pasted on to the phase image (**b**). Then, the cortical region on the phase image (**b**) was divided into three sub-regions of roughly equal area (front, middle, and back), so did the medulla. SWI, susceptibility-weighted imaging.

Statistical analysis

For statistical analysis, SPSS 22.0 software (IBM, Armonk, NY, USA) was used. The data were expressed as the median (interquartile range) (M [Q1 and Q3]) and the Mann–Whitney U test was used to compare the difference in the ARV between the two groups. Kruskal–Wallis test was used to compare the difference in the ARV among multiple groups. An independent sample *t*-test was used to compare the difference of the renal iron content measured by the atomic absorption spectrophotometer between the two groups. Analysis of variance was used to compare the difference of the renal iron content measured by the atomic absorption spectrophotometer among multiple groups. Spearman rank correlation analysis was used to analyze the correlation between the angle radian values and the renal iron content measured by the atomic absorption spectrophotometer. The symbol r was used to represent the correlation coefficient.[16] The correlation was interpreted as follows: $r > 0$ was considered a positive correlation; $r < 0$ was considered a negative correlation; $|r| = 1$ was considered a perfect correlation; $0.7 \leq |r| < 1$ was considered a high correlation; $0.4 \leq |r| < 0.7$ was considered a moderate correlation; $0 \leq |r| < 0.4$ was considered a low correlation; and $r = 0$ was considered zero correlation.[16] $P < 0.05$ was considered statistically significant.

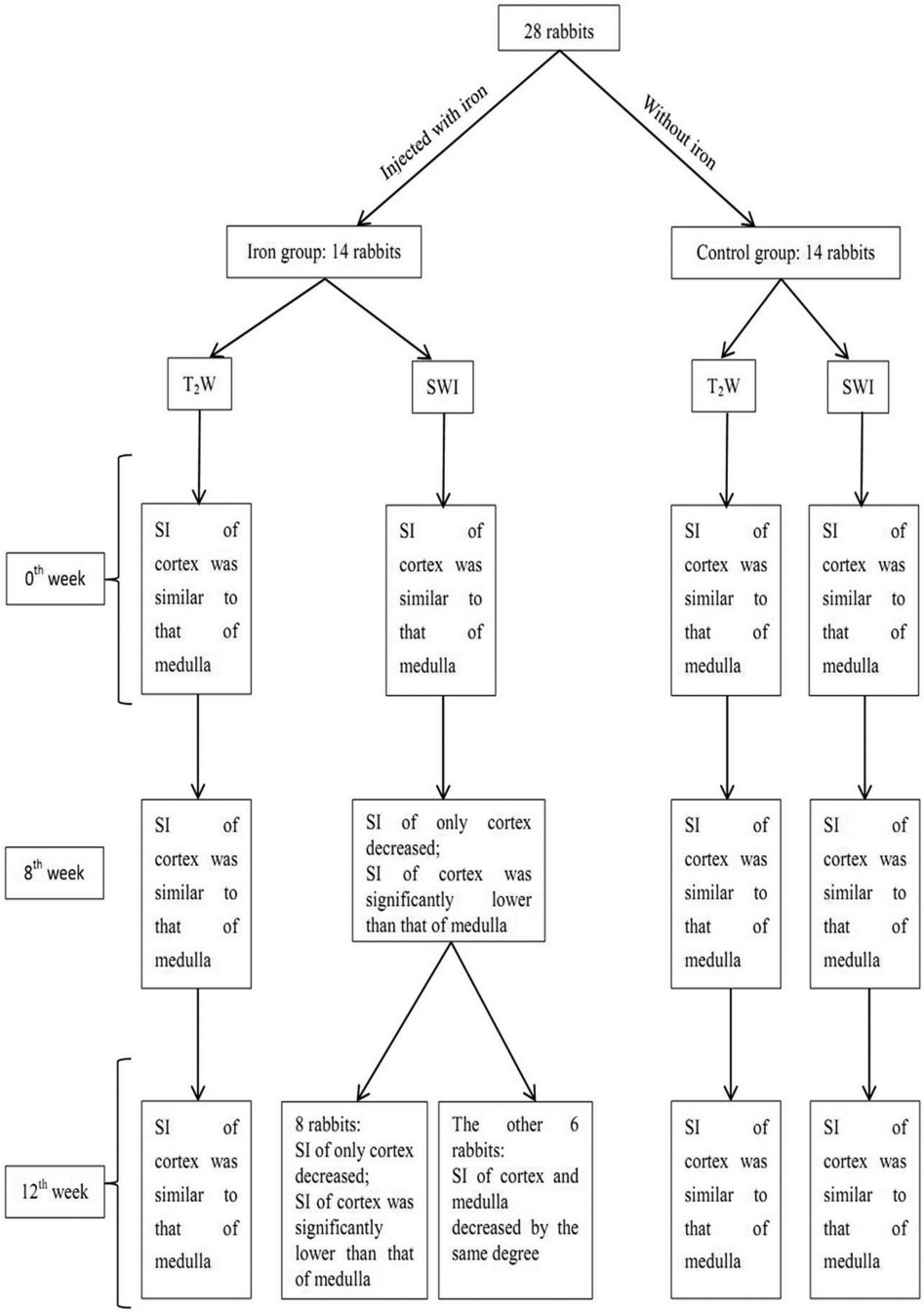

Fig. 2 The flowchart shows the change in SI for the renal cortex and medulla on T_2WI and SWI images in the control and iron agent group at different time points. SI, signal intensity; SWI, susceptibility-weighted imaging; T_2W, T_2-weighted; T_2WI, T_2-weighted image.

Results

Qualitative analysis

The flowchart of change in SI for the renal cortex and medulla on T_2WI and SWI is summarized in Fig. 2.

At the 0th week (Fig. 3): in the control group, for all rabbits, the SI of cortex was similar to that of medulla on both T_2WI and SWI, respectively; even in the iron group, for all rabbits, the SI of cortex was similar to that of medulla on both T_2WI and SWI, respectively; there was no significant change in the SI of cortex on both T_2WI and SWI between the control and iron group, so did the medullary region; in the control and iron group, there was no significant change in the SI of cortex on both T_2WI

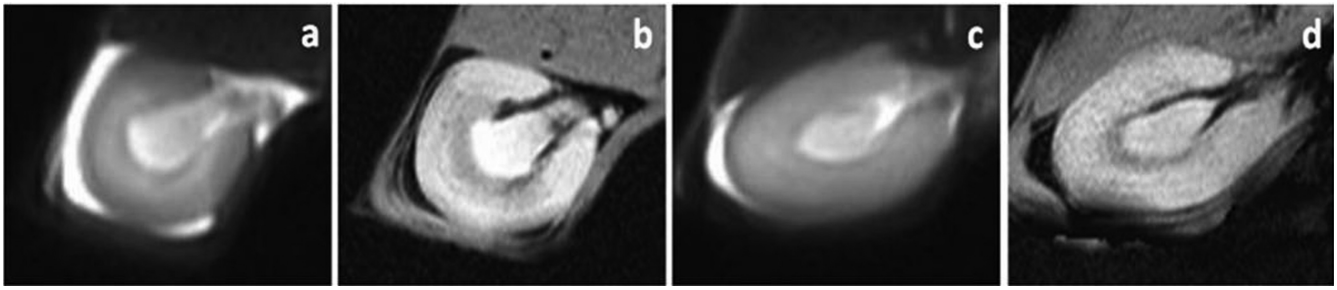

Fig. 3 At the 0th week, the control (**a** and **b**) and iron (**c** and **d**) group. In the control group (**a** and **b**), the SI of cortex was similar to that of medulla on both T_2WI (**a**) and SWI (**b**) images, respectively. In the iron group (**c** and **d**), the SI of cortex was similar to that of medulla on both T_2WI (**c**) and SWI (**d**) images, respectively, too. There was no significant change in the SI of cortex on both T_2WI (**a** vs. **c**) and SWI (**b** vs. **d**) images between the control and iron group, so did the medulla. SI, signal intensity; SWI, susceptibility-weighted imaging; T_2WI, T_2-weighted image.

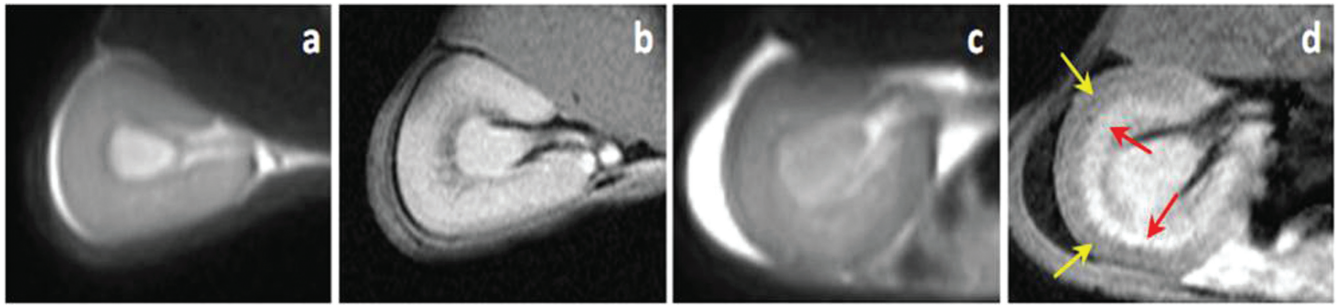

Fig. 4 In the 8th week, the control (**a** and **b**) and iron (**c** and **d**) group. In the control group (**a** and **b**), the SI of cortex was similar to that of medulla on both T_2WI (**a**) and SWI (**b**) images, respectively. In the iron group (**c** and **d**), the SI of cortex was similar to that of medulla on T_2WI (**c**) images, but the SI of cortex (yellow arrows) was significantly lower than that of the medulla (red arrows) on SWI (**d**) images. There was no significant change in the SI of cortex on T_2WI (**a** vs. **c**) images between the control and iron group, so did the medullary. On SWI images (**d** vs. **b**), the SI of cortex in the iron group was significantly lower than that in the control group, however, there was no significant change in the SI of medullary between the control and iron group. SI, signal intensity; SWI, susceptibility-weighted imaging; T_2WI,T_2-weighted image.

and SWI between the males and females, so did the medulla.

At the 8th week (Fig. 4): in the control group, for all rabbits, the SI of cortex was similar to that of medulla on both T_2WI and SWI, respectively; in the iron group, for all rabbits, the SI of cortex was similar to that of medulla on T_2WI; however, the SI of cortex was significantly lower than that of the medulla on SWI; there was no significant change in the SI of cortex on T_2WI between the control and iron group, so did the medullary region; on SWI, the SI of cortex in the iron group was significantly lower than the control group; however, there was no significant change in the SI of medullary region between the control and iron group; in the control and iron group, there was no significant change in the SI of cortex on both T_2WI and SWI between the males and females, so did the medulla.

At the 12th week (Fig. 5): in the control group, for all rabbits, the SI of cortex was similar to that of medulla on both T_2WI and SWI; in the iron group, for all rabbits, the SI of cortex was similar to that of medulla on T_2WI; in the iron group, on SWI images, eight rabbits were found to have decreased SI of only cortex, and the other six rabbits had decreased SI of cortex and medulla by the same degree; there was no significant change in the SI of cortex on T_2WI between the control and iron group, so did the medullary region; on SWI, the SI of cortex in the iron group was significantly lower than the control group; in the control and iron group, there was no significant change in the SI of cortex on both T_2WI and SWI between the males and females, so did the medulla.

Quantitative analysis

In the control group, there was no significant difference in the ARV of the renal cortex among the imaging evaluation done in the 0th, 8th, and 12th week (Table 2), so did the renal medulla.

In the iron group: For renal cortex, there was a significant difference in the ARV among the 0th, 8th, and 12th week; the ARV of the 8th and 12th week were significantly higher than that of the 0th week; there was no significant difference in the ARV between the 8th and 12th week (Table 2). For renal medulla, there was a significant

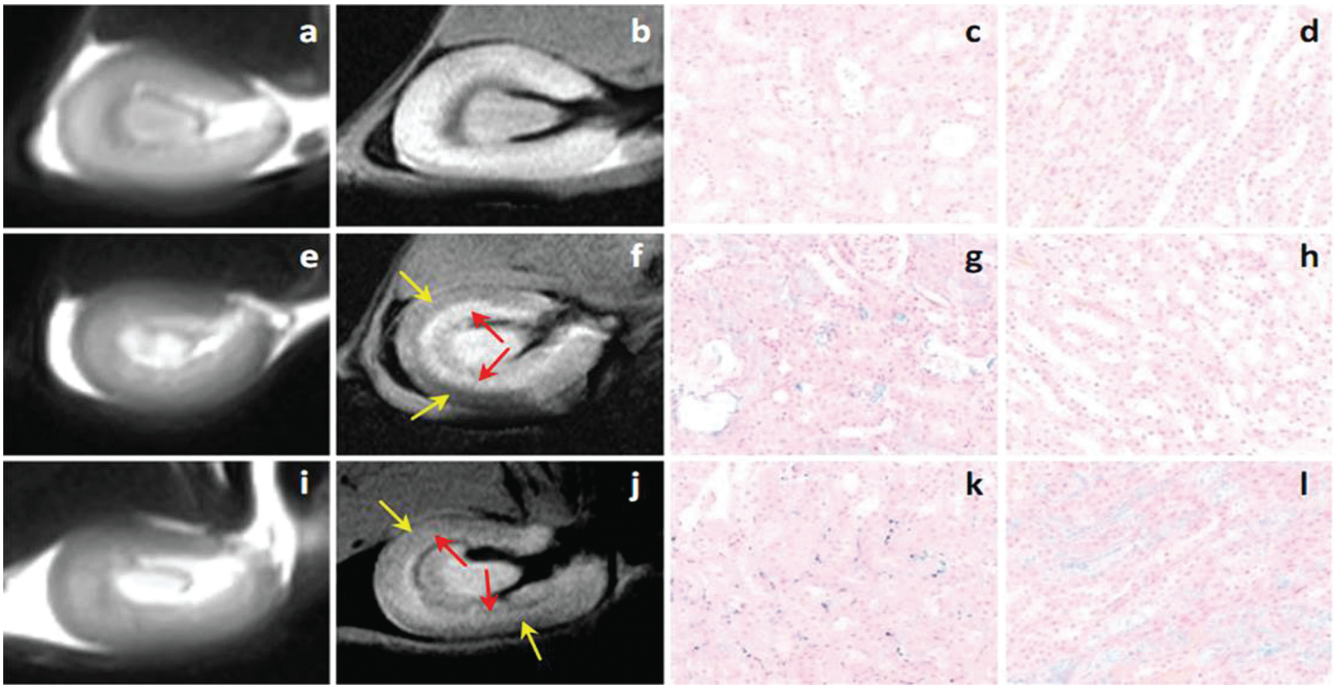

Fig. 5 In the 12th week, the control group (**a-d**), the iron group (**e-h**) with only cortical SI decreased, and the iron group (**i-l**) with cortical and medullary SI both decreased. In the control group (**a-d**): the SI of cortex was similar to that of medulla on both T_2WI (**a**) and SWI (**b**) images, respectively, and Photomicrograph showed no blue-positive irons deposit in both renal cortex (**c**) and medulla (**d**) (Prussian blue stain, × 400). In the iron group (**e-h**) with only cortical SI decreased: the SI of cortex was similar to that of medulla on T_2WI (**e**) images, but the SI of cortex (yellow arrows) was significantly lower than that of the medulla (red arrows) on SWI (**f**) images; photomicrograph showed many blue-positive irons deposit in the renal cortex (**g**) but no deposit in the medulla (**h**) (Prussian blue stain, × 400). In the iron group (**i-l**) with cortical and medullary SI all decreased: the SI of cortex was similar to that of medulla on T_2WI (**i**) images, and the SI of cortex (yellow arrows) and medulla (red arrows) were both decreased on SWI (**j**) images. Photomicrograph showed many blue-positive irons deposit in both cortex (**k**) and medulla (**l**) (Prussian blue stain, × 400). SI, signal intensity; SWI, susceptibility-weighted imaging; T_2WI, T_2-weighted image.

Table 2 Comparison of the difference in the angle radian value of renal cortex between the control and iron group

Group	n	0th week	8th week	12th week	H	*P*
Control	14	–0.0199 (–0.0469, –0.0002)	–0.0219 (–0.0546, –0.0015)	–0.0242 (–0.0549, –0.0109)	0.592	0.744
Iron	14	–0.0317 (–0.0481, –0.0108)	0.2024 (0.1639, 0.2796)*	0.2610 (0.2221, 0.3252)*	29.793	0.000
Z		–0.804	–4.503	–4.503		
P		0.421	0.000	0.000		

Data were expressed as M (Q1 and Q3). * No significant difference. M, median; Q1, first quartile; Q3, third quartile.

difference in the ARV among the 0th, 8th, and 12th week; the ARV of the other six rabbits that had decreased SI of cortex and medulla by the same degree in the 12th week was significantly higher than that of the 0th week, 8th week, and eight rabbits that found to have decreased SI of only cortex in the 12th week (Table 3).

Between the iron and control group: For renal cortex, there was no significant difference in the ARV at 0th week (Table 2); in the 8th and 12th week, the ARV of the iron group was significantly higher than that of the control group, respectively (Table 2). For renal medulla, there was no significant difference in the ARV at the 0th and 8th week; in the 12th week, there was no significant difference in the ARV between eight rabbits that found to have decreased SI of only cortex and the control group, but the ARV of the other six rabbits which had decreased SI of cortex and medulla by the same degree in the iron group was significantly higher than that of the control group (Table 3).

Between the cortex and medulla: In the control group at the 0th, 8th, and 12th week, there was no significant difference in the ARV between the cortex and medulla (Table 4). In the iron group at the 0th week, there was no significant difference in the ARV between cortex and

Table 3 Comparison of the difference in the angle radian value of renal medulla between the control and iron group.

Group	n	0th week	8th week	12th week		H	*P*
Control	14	–0.0188 (–0.0435, –0.0071)	–0.0224 (–0.0530, –0.0016)	–0.0274 (–0.0556, –0.0115)		0.832	0.660
Iron	14	–0.0278(–0.0450, –0.0103)*	–0.0107 (–0.0476, 0.0003)*	–0.0190 (–0.0404, -0.0152)*, *[1]	0.2858 (0.2382, 0.3457) *[2]	15.683	0.001
Z		–0.689	–0.322	–1.024	–3.464		
P		0.491	0.748	0.306	0.001		

Data were expressed as M (Q1, Q3). * No significant difference. *[1] Eight rabbits were found to have decreased SI of only cortex. *[2] The other six rabbits had decreased SI of cortex and medulla by the same degree. M, median; Q1, first quartile; Q3, third quartile; SI, signal intensity.

Table 4 Comparison of the difference in the angle radian value of between the cortex and medulla in the control and iron group.

Kidney	n	0th week		8th week		12th week		
		Control	Iron	Control	Iron	Control	Iron	
Cortex	14	–0.0199 (–0.0469, –0.0002)	–0.0317 (–0.0481, –0.0108)	–0.0219 (–0.0546, –0.0015)	0.2024 (0.1639, 0.2796)	–0.0242 (–0.0549, –0.0109)	0.2610 (0.2221, 0.3252)	
Medulla	14	–0.0188 (–0.0435, –0.0071)	–0.0278 (–0.0450, –0.0103)	–0.0224 (–0.0530, –0.0016)	–0.0107 (–0.0476, 0.0003)	–0.0274 (–0.0556, –0.0115)	–0.0190 (–0.0404, –0.0152)*[1]	0.2858 (0.2382, 0.3457)*[2]
Z		–0.230	–0.345	–0.161	–4.503	–0.207	–3.822	–0.784
P		0.818	0.730	0.872	0.000	0.836	0.000	0.433

Data were expressed as M (Q1 and Q3). *[1] Eight rabbits were found to have decreased SI of only cortex. *[2] The other six rabbits had decreased SI of cortex and medulla by the same degree. M, median; Q1, first quartile; Q3, third quartile; SI, signal intensity.

medulla; in the iron group at the 8th week, the ARV of renal cortex was significantly higher than that of medulla; in the iron group at the 12th week, the ARV of renal cortex was significantly higher than that of the medulla of the eight rabbits that were found to have decreased SI of only cortex, and there was no significant difference in the ARV between the cortex and the medulla of the other six rabbits that had decreased SI of cortex and medulla by the same degree

Between the male and female: There was no significant difference in the ARV of cortex and medulla in the control group at the 0th, 8th, and 12th week, respectively (Table 5), so did in the iron group (Table 6).

Hematoxylin-eosin stain

At the 12th week: in the control group, the renal cortex and medulla were clearly demarcated, the structures of glomerular capillaries were clear, and the structures of renal tubular epithelial cells were normal; in the iron group, part of cortex, medulla, and interstitial congestion, the renal tubular epithelial cells were edema and degeneration; brownish-yellow deposits can be seen in renal tubular epithelial cells (Prussian blue stain confirmed that hemosiderin has accumulated in the cells).

Prussian blue stain

At the 12th w: in the control group, none of the rabbits had blue-positive iron deposit either in the renal cortex or medulla; in the iron group, eight rabbits were found to have many Prussian blue-positive irons (which represented hemosiderin particles) deposit in the renal cortex; however, none of them had a deposit in the medulla, and the other six rabbits were found to have many Prussian blue-positive irons (which represented hemosiderin particles) deposit both in the cortex and medulla (Fig. 5).

Atomic absorption spectrophotometer evaluation

At the 12th week: the iron content in the renal cortex that was measured by the atomic absorption spectrophotometer in the iron group was significantly higher than that of the control group; the iron content in the renal medulla of the other six rabbits that had decreased SI of cortex and medulla by the same degree in the iron group was significantly higher than that of the control group; in the control group, there was no significant difference in the iron content between the cortex and medulla; in the iron group, there was a significant difference in the iron content among the cortex, medulla of eight rabbits, and medulla of the other six rabbits (Table 7).

Table 5 Comparison of the difference in the angle radian value of between male and female in the control group.

Sex	n	0th week		8th week		12th week	
		Cortex	Medulla	Cortex	Medulla	Cortex	Medulla
Male	7	–0.0172 (–0.0364, –0.0087)	–0.0147 (–0.0345, 0.0039)	–0.0327 (–0.0595, –0.0011)	–0.0151 (–0.0334, 0.0029)	–0.0195(–0.0714, –0.0142)	–0.0219 (–0.0513, –0.0137)
Female	7	–0.0226 (–0.0548, –0.0031)	–0.0248(–0.0505, –0.0083)	–0.0110 (–0.0529, –0.0016)	–0.0357 (–0.0540, –0.0055)	–0.0347 (–0.0512, –0.0022)	–0.0382 (–0.0649, –0.0056)
Z		–0.447	–1.214	–0.064	–0.958	–0.575	–0.192
P		0.655	0.225	0.949	0.338	0.565	0.848

Data were expressed as M (Q1 and Q3). M, median; Q1, first quartile; Q3, third quartile.

Table 6 Comparison of the difference in the angle radian value of between male and female in the iron group.

Sex	n	0th week		8th week		12th week	
		Cortex	Medulla	Cortex	Medulla	Cortex	Medulla
Male	9	–0.0226 (–0.0395, –0.0106)	–0.0209 (–0.0501, 0.0101)	0.2003 (0.1371, 0.2382)	–0.0069 (–0.0475, 0.0014)	0.2591.(0.2089, 0.3257)	0.0262 (–0.0341, 0.3296)
Female	5	–0.0437 (–0.0600, –0.0115)	–0.0373(–0.0463, –0.0066)	0.2660 (0.2018, 0.3165)	–0.0376(–0.0506, –0.0122)	0.3006 (0.2238, 0.3303)	–0.0027 (–0.0401, 0.2485)
Z		–1.133	–0.200	–1.533	–0.333	–0.467	–0.600
P		0.257	0.841	0.125	0.739	0.641	0.549

Data were expressed as M (Q1 and Q3). M, median; Q1, first quartile; Q3, third quartile.

Table 7 Comparison of the difference in the iron content measured by the atomic absorption spectrophotometer at the 12th week.

Group	n	Cortex (mg/kg)	Medulla (mg/kg)		Statistics	*P*
Control	14	71.97 ± 9.42	73.44 ± 11.52		*t* = –0.370	0.714
Iron	14	137.38 ± 12.32*	72.73 ± 13.80*[1]	137.08 ± 9.73*,*[2]	*F* = 78.802	0.000
t		–15.784	0.131	–11.803		
P		0.000	0.897	0.000		

* No significant difference. *[1] Eight rabbits were found to have decreased SI of only cortex. *[2] The other six rabbits had decreased signal intensity of cortex and medulla by the same degree.

Correlation between the ARV and the iron content measured by the atomic absorption spectrophotometer

At the 12th week, for all rabbits, the ARV of renal cortex and medulla was highly positively correlated with the iron content measured by atomic absorption spectrophotometer (r = 0.773, P = 0.000).

Discussion

In this study, we evaluated both the control and iron group with MRI and SWI in the 0th, 8th, and 12th week, respectively. Through this comparative study, it was found that excessive deposition of iron can lead to a decrease in SWI SI; however, there was no obvious change in conventional MRI SI. Through SWI evaluation, excess iron deposition was noticed mainly in the renal cortex at the 8th week, and in the renal cortex or medulla at the 12th week. The ARV calculated from the phase images can be used to quantitatively evaluate the excess iron deposition in the renal cortex and medulla. There was no significant difference between the results of qualitative and quantitative analysis (ARV) of SWI and rabbits' sex in the control and iron group. The ARV was highly positively correlated with the iron content measured by atomic absorption spectrophotometer. The results of the hematoxylin-eosin stain, Prussian blue stain, and atomic absorption photometer further verified the findings of SWI.

Our study indicated that it is feasible to evaluate excess iron deposition in the kidney through SWI.

Iron overload results in an increase in storage iron[17] and has been recognized as a risk factor for organ dysfunction.[4] Excess iron causes kidney damage in patients through a combination of oxidative stress.[2,17,18] Regular monitoring of iron deposition in the kidneys of patients is of great significance for managing kidney injury.[18] SWI is a high-resolution and full-flow-compensated gradient echo sequence that uses tissue magnetic susceptibility differences to produce contrast and improving the sensitivity to detect iron and other substances that affect local magnetic fields.[12] We have used SWI for the first time to detect excess iron deposition in the kidney.

In renal tissue, excess iron is stored in the form of ferritin.[13] Ferritin, as a strong magnetic substance, aligns along the main magnetic field on SWI producing a larger field, which can cause voxels to phase shift, resulting in phase differences in the area and magnetically sensitive signals uneven.[13,19] This study found no significant difference in the SWI SI between the renal cortex and medulla without iron injection. However, after the iron injection: in the 8th week, in all rabbits, the SWI SI of cortex was significantly lower than that of medulla; by comparison, at the 12th week, eight of them were found to have the SWI SI of cortex lower than that of the medulla, while the SI of cortex and medulla of the other six rabbits decreased to the same extent.

In the iron group in the 12th week, the SWI results showed the excess iron of eight rabbits was mainly deposited in the renal cortex, and the excess iron of the other six rabbits was deposited in both the renal cortex and the medulla, which was consistent with the results of Prussian blue staining. We speculate that the metabolism of excess iron in the body was very complicated, which may cause this difference in the same group. Another possible reason was that the deposition of excess iron in the kidney was related to the time. Depending on the selected time point, excess iron deposition in the renal cortex and medulla may be different. Fortunately, SWI can accurately detect the difference of iron deposition in the same group.

With the increasing iron content in the tissue, the phase difference is greater.[13,19] Any change in iron content will cause a change in the phase of the tissue relative to its surroundings. In this study, excess iron was deposited in the renal cortex or medulla. The more iron deposited in the cortex or medulla, the greater the unevenness of the magnetic field, and the decrease in SWI SI of cortex or medulla was more significant. Some studies have demonstrated that iron overload can damage the kidney.[7,8,20] Iron, as a catalyst, can promote the highly reactive free radical generation in the Fenton reaction, and excessive iron deposition produces excessive highly reactive radicals, which can damage renal tubular epithelial cells.[7,8]

The phase value can be used as a means to quantify iron content in the normal and abnormal circumstances.[21,22] In the phase image, there is a phase difference between the human tissues with iron deposition and those without iron deposition, so the contrast is significantly enhanced.[23] Gao et al.[13] proved that there is a high correlation between the iron content in the tissue and the phase value. The average phase value of each ROI measured on the phase image had a significant negative correlation with the tissue iron content. In this study, we have used ARV as a quantitative value for iron deposition. According to the calculation, the ARV had a negative correlation with the phase value and a significant positive correlation with the iron content of the tissue. In the 12th week, the ARV of the renal cortex in the iron group was significantly higher than that of the control group, showing that the iron deposition in the former was significantly higher than that of the latter. This was consistent with the results of Prussian blue staining and atomic absorption spectrophotometer, respectively. In the 12th week, Prussian blue staining showed that iron deposition was significant in the iron group. However, no positive staining was noted in the control group, and the atomic absorption spectrophotometer showed the iron content of the renal cortex in the iron group was significantly higher than that in the control group. Moreover, SWI had been proved to identify abnormal iron accumulation in the tissue in the previous study.[10] In the present study, it was further verified pathologically that SWI can quantitatively evaluate the excess iron deposition in the kidney.

In this experiment, rabbits were injected with a certain amount of iron, and the deposition of excess iron was noticed in the renal cortex or medulla. At the same time, SWI and T_2WI were used for qualitative observation. It was found that the SI of the renal cortex or medulla on SWI was significantly reduced, while that on T_2WI remained unchanged. It shows that SWI was significantly better than T_2WI in evaluating renal excess iron deposition. This was possible as the SWI, a novel MRI modality, uses a different technique from traditional spin-density, T_1, or T_2 imaging recalled echo pulse sequence to acquire data.[24] In other studies, SWI was found to be more sensitive for assessing the iron than other techniques, such as T_2WI, and T_2^*WI.[10,25]

This study had the following shortcomings: (1) Magnetically sensitive artifacts may affect the measurement of cortical phase value. During MRI scanning, magnetically sensitive artifacts mainly arise from two aspects: one was that the rabbits still had a slight breathing movement even after anesthesia administration; the other was that the kidneys of these rabbits were affected by overlapping intestinal gas. (2) The left kidneys alone were selected for the study; however, the right kidneys were not evaluated at the same time. The rationale for this selection was that: First, in the preliminary experiment, we repeatedly found that the magnetic sensitivity artifacts of the right kidneys were relatively heavy and quality of the images was poor. It may be related to the anatomy of the right kidney being closer to the lower edge of the ribs and more affected by the gas in the intestine. Second, after scanning the left kidney, the right kidney was scanned next, requiring a supplemental dosage of anesthetic agents. However, an excessive amount of anesthetic was harmful and even caused death. (3) The kidney tissue might not be negligible when iron content is smaller. Although the ARV can be used to quantitatively assess the excess iron deposition in the kidney, it may not be

converted into the absolute value of iron content at present. Our study is a preliminary research. Further studies on more samples will be needed in the future.

Conclusion

It is feasible that SWI can be used non-invasively to evaluate the excess iron deposition in the kidney. The excess iron mainly deposits in the renal cortex or medulla, causing their SWI SI to decrease. The ARV calculated with phase images can be used for quantitative analysis of excess iron deposition in the renal cortex and medulla. Our study provides an experimental and theoretical basis for the future application of SWI in iron overload of CKD.

Funding

This work was supported by the National Natural Science Foundation of China (grant numbers 81771798) and Major Science and Technology Program of Changzhou Municipal Health and Family Planning Commission (grant numbers ZD201806).

Conflicts of Interest

The authors declare that they have no conflicts of interest.

References

1. Liu S, Wang C, Zhang X, et al. Quantification of liver iron concentration using the apparent susceptibility of hepatic vessels. Quant Imaging Med Surg 2018; 8:123–134.
2. Ikeda Y, Enomoto H, Tajima S, et al. Dietary iron restriction inhibits progression of diabetic nephropathy in db/db mice. Am J Physiol Renal Physiol 2013; 304:F1028–1036.
3. Grassedonio E, Meloni A, Positano V, et al. Quantitative $T2^*$ magnetic resonance imaging for renal iron overload assessment: normal values by age and sex. Abdom Imaging 2015; 40:1700–1704.
4. Ige AO, Ongele FA, Adele BO, et al. Pathophysiology of iron overload-induced renal injury and dysfunction: Roles of renal oxidative stress and systemic inflammatory mediators. Pathophysiology 2019; 26:175–180.
5. Naito Y, Fujii A, Sawada H, et al. Dietary iron restriction prevents further deterioration of renal damage in a chronic kidney disease rat model. J Hypertens 2013; 31:1203–1213.
6. Ikeda Y, Horinouchi Y, Hamano H, et al. Dietary iron restriction alleviates renal tubulointerstitial injury induced by protein overload in mice. Sci Rep 2017; 7:10621.
7. van Raaij S, van Swelm R, Bouman K, et al. Tubular iron deposition and iron handling proteins in human healthy kidney and chronic kidney disease. Sci Rep 2018; 8:9353.
8. Naito Y, Fujii A, Sawada H, et al. Association between renal iron accumulation and renal interstitial fibrosis in a rat model of chronic kidney disease. Hypertens Res 2015; 38:463–470.
9. Kang H, Han M, Xue J, et al. Renal clearable nanochelators for iron overload therapy. Nat Commun 2019; 10:5134.
10. Hasiloglu ZI, Asik M, Ure E, et al. The utility of susceptibility-weighted imaging to evaluate the extent of iron accumulation in the choroid plexus of patients with β-thalassaemia major. Clin Radiol 2017; 72:903.e1–903.e7.
11. Li RK, Zeng MS, Qiang JW, et al. Improving detection of iron deposition in cirrhotic liver using susceptibility-weighted imaging with emphasis on histopathological correlation. J Comput Assist Tomogr 2017; 41:18–24.
12. Park M, Moon Y, Han SH, et al. Motor cortex hypointensity on susceptibility-weighted imaging: a potential imaging marker of iron accumulation in patients with cognitive impairment. Neuroradiology 2019; 61:675–683.
13. Gao L, Jiang Z, Cai Z, et al. Brain iron deposition analysis using susceptibility weighted imaging and its association with body iron level in patients with mild cognitive impairment. Mol Med Rep 2017; 16:8209–8215.
14. Chen L, Wei X, Liu C, et al. Brain iron deposition in primary insomnia-An in vivo susceptibility-weighted imaging study. Brain Behav 2019; 9:e01138.
15. Lu L, Cao H, Wei X, et al. Iron deposition is positively related to cognitive impairment in patients with chronic mild traumatic brain injury: assessment with susceptibility weighted imaging. Biomed Res Int 2015; 2015:470676.
16. Sun J, Yu S, Chen J, et al. Assessment of delayed graft function using susceptibility-weighted imaging in the early period after kidney transplantation: a feasibility study. Abdom Radiol (NY) 2019; 44:218–226.
17. Gao W, Li X, Gao Z, et al. Iron increases diabetes-induced kidney injury and oxidative stress in rats. Biol Trace Elem Res 2014; 160:368–375.
18. Chaudhary K, Chilakala A, Ananth S, et al. Renal iron accelerates the progression of diabetic nephropathy in the HFE gene knockout mouse model of iron overload. Am J Physiol Renal Physiol 2019; 317:F512–F517.
19. Haacke EM, Makki M, Ge Y, et al. Characterizing iron deposition in multiple sclerosis lesions using susceptibility weighted imaging. J Magn Reson Imaging 2009; 29:537–544.
20. Ahmadzadeh A, Jalali A, Assar S, et al. Renal tubular dysfunction in pediatric patients with beta-thalassemia major. Saudi J Kidney Dis Transpl 2011; 22:497–500.
21. Haacke EM, Ayaz M, Khan A, et al. Establishing a baseline phase behavior in magnetic resonance imaging to determine normal vs. abnormal iron content in the brain. J Magn Reson Imaging 2007; 26:256–264.
22. Hagemeier J, Heininen-Brown M, Poloni GU, et al. Iron deposition in multiple sclerosis lesions measured by susceptibility-weighted imaging filtered phase: a case control study. J Magn Reson Imaging 2012; 36:73–83.
23. Haacke EM, Cheng NY, House MJ, et al. Imaging iron stores in the brain using magnetic resonance imaging. Magn Reson Imaging 2005; 23:1–25.
24. Pietracupa S, Martin-Bastida A, Piccini P. Iron metabolism and its detection through MRI in parkinsonian disorders: a systematic review. Neurol Sci 2017; 38:2095–2101.
25. Li SJ, Ren YD, Li J, et al. The role of iron in Parkinson's disease monkeys assessed by susceptibility weighted imaging and inductively coupled plasma mass spectrometry. Life Sci 2020; 240:117091.